LEGIBILITY NOTICE

A major purpose of the Technical Information Center is to provide the broadest dissemination possible of information contained in DOE's Research and Development Reports to business, industry, the academic community, and federal, state and local governments.

Although a small portion of this report is not reproducible, it is being made available to expedite the availability of information on the research discussed herein.

LA-UR -88-229

Los Alamos National Laboratory is operated by the University of California for the United States Department of Energy under contract W-7405-ENG-36

TITLE BOLTZMANN-FOKKER-PLANCK CALCULATIONS USING STANDARD DISCRETE-ORDINATES CODES

LA-UR--88-229

DE88 005393

AUTHOR(S) Jim E. Morel, X-6

SUBMITTED TO To be published in proceedings of the conference on "Computational Methods in High Temperature Physics," held at LANL, Feb. 2-6, 1987.

DISCLAIMER

Los Alamos National Laboratory
Los Alamos, New Mexico 87545

BOLTZMANN-FOKKER-PLANCK CALCULATIONS USING STANDARD DISCRETE-ORDINATES CODES

by

J. E. Morel
Radiation Transport Group, X-6
Applied Theoretical Physics Division
Los Alamos National Laboratory

ABSTRACT

The Boltzmann-Fokker-Planck (BFP) equation can be used to describe both neutral and charged-particle transport. Over the past several years, the author and several collaborators have developed methods for representing Fokker-Planck operators with standard multigroup-Legendre cross-section data. When these data are input to a standard S_n code such as ONETRAN, the code actually solves the Boltzmann-Fokker-Planck equation rather than the Boltzmann equation. This is achieved without any modification to the S_n codes. Because BFP calculations can be more demanding from a numerical viewpoint than standard neutronics calculations, we have found it useful to implement new quadrature methods and convergence acceleration methods in the standard discrete-ordinates code, ONETRAN. We discuss our BFP cross-section representation techniques, our improved quadrature and acceleration techniques, and present results from BFP coupled electron-photon transport calculations performed with ONETRAN.

I. INTRODUCTION

Fokker-Planck operators are asymptotic approximations to the Boltzmann scattering operator that apply in the forward-peaked elastic scattering limit.[1] Highly forward-peaked scattering kernels are often quite difficult to numerically approximate, whereas Fokker-Planck operators, which are differential operators, can often be approximated using straightforward differencing techniques. Hence charged-particle transport, which is dominated by highly forward-peaked elastic coulomb scattering, is often described with a transport equation that has Boltzmann operators describing the "large-angle" scattering and Fokker-Planck operators describing the "small-angle" scattering. Such an equation is known as a Boltzmann-Fokker-Planck (BFP) equation. Much attention has been given to BFP equations over the last several years.[1,2,3] These equations have been used for both charged-particle and neutral-particle transport calculations. Several years ago, we demonstrated that the Fokker-Planck equation for charged-particles transporting in fully-ionized plasmas can be solved in 1-D slab and spherical geometries using standard discrete-ordinates codes.[1] No code modifications are necessary. The Fokker Planck operators are represented in terms of multigroup-Legendre cross-section coefficients. Thus, one need simply input appropriate cross-section data to perform a Fokker-Planck calculation. Over the last several years, we have been investigating the generalization of existing discrete-ordinates codes to allow both Fokker-Planck and Boltzmann-Fokker-Planck calculations in all geometries. In addition, we have sought to improve our multigroup cross-section representations for the Fokker-Planck operators. The purpose of this paper is to briefly review our Fokker-Planck operator representations and the new S_n methods that we have developed, and to demonstrate the effectiveness of our approach when applied to coupled electron-photon transport calculations.

II. MULTIGROUP REPRESENTATIONS FOR FOKKER-PLANCK OPERATORS

In this section we derive simple representations for two Fokker-Planck operators. Our primary purpose is to convey the basic approach used in deriving such representations. A Fokker-Planck equation that can be used to describe the transport of charged-particles in plasmas is given by:[1]

$$\mu \frac{\partial}{\partial z}\psi = \frac{\alpha}{2}\frac{\partial}{\partial \mu}\left[(1-\mu^2)\frac{\partial}{\partial \mu}\psi\right] + \frac{\partial}{\partial E}(S\psi) + Q \quad , \tag{1}$$

where z is the space coordinate, μ is the direction cosine of the transport particle relative to the z-axis, ψ is the angular flux, α is the momentum transfer, S is the stopping power, and Q is the source function. We refer to the Fokker Planck angular and energy operators in Eq. (1) as the angular diffusion (AD) operator and the continuous slowing down (CSD) operator, respectively. The AD operator approximates the Boltzmann scattering operator in the limit as the scattering cross section goes to infinity, and the average cosine of the scattering angle goes to unity in such a way that the average change in the particle direction per unit pathlength is constant and is given by the momentum transfer (steradians/pathlength). The

momentum transfer is commonly referred to as the transport-corrected cross section in the neutron transport literature. The AD operator causes a particle to continuously diffuse in direction space rather than discretely scatter. The CSD operator approximates the Boltzmann scattering operator in the limit as the scattering cross section goes to infinity and the average energy loss per unit pathlength goes to zero in such a way that the average energy loss per unit pathlength remains constant and is given by the stopping power (energy/pathlength). The CSD operator causes a particle to continuously lose energy rather than lose it in discrete-scattering events.

The multigroup Boltzmann equation solved by standard discrete-ordinates codes is:[4]

$$\mu_m \frac{\partial}{\partial z}\psi_{m,g} + \sigma_{t,g}\psi_{m,g} = \left[\sum_{k=1}^{G}\sum_{\ell=0}^{L}(2\ell+1)\,\sigma_{k\to g,\ell}\Phi_{k,\ell}P_\ell(\mu_m)\right] + Q_{g,m} \quad , \quad m = 1,N \quad , \quad g = 1,G \quad , \tag{2}$$

where m is the direction index, g is the group index, N is the total number of directions, G is the total number of groups, L is the degree of the Legendre cross-section expansion, $\sigma_{t,g}$ is the total cross section for group g, $\sigma_{k\to g,\ell}$ is the ℓ'th Legendre moment of the cross section for scattering from group k to group g, $\Phi_{k,\ell}$ is the ℓ'th Legendre moment of the angular flux for group k, and $P_\ell(x)$ is the Legendre polynomial of degree ℓ. To solve Eq. (1) using Eq. (2), we must appropriately define the cross-section coefficients. We first consider the AD operator. Note that this operator changes the particle direction, but not the particle energy. Thus, the cross-section coefficients corresponding to this operator must be within-group scattering coefficients. The key to approximating the AD operator with the Boltzmann scattering operator is found because both of these operators have the same eigenfunctions, namely, the Legendre polynomials:

$$\frac{\alpha}{2}\frac{\partial}{\partial\mu}\left[(1-\mu^2)\,\frac{\partial}{\partial\mu}P_\ell(\mu)\right] = -\frac{\alpha}{2}\ell(\ell+1)\,P_\ell(\mu) \quad , \tag{3}$$

$$\int_{-1}^{+1}\sigma_s(\mu_0)\,P_\ell(\mu')\,d\mu' - \sigma_s P_\ell(\mu) = -(\sigma_0-\sigma_\ell)\,P_\ell(\mu) \quad . \tag{4}$$

Legendre expansion coefficients for the AD operator are obtained by equating the eigenvalues in Eqs. (3) and (4):

$$\sigma_0 - \sigma_\ell = \frac{\alpha}{2}\ell(\ell+1) \quad , \quad \ell = 0,L \quad . \tag{5}$$

The difference between the zero'th and ℓ'th moments is defined by Eq. (5); but to obtain a specific definition for each moment, we must define σ_0. The value of σ_0 can be arbitrarily chosen; but to ensure stability in the source iteration process, it is required that

$$|\sigma_\ell| \le \sigma_0 \quad , \quad \ell = 0,L \quad . \tag{6}$$

A simple definition that satisfies Eq. (6) can be obtained by requiring that σ_ℓ be zero. Specifically, this requirement gives:

$$\sigma_0 = \frac{\alpha}{2}L(L+1) \quad . \tag{7}$$

From Eqs. (5) and (7) we obtain the desired definition for each moment:

$$\sigma_\ell = \frac{\alpha}{2}\left[L(L+1) - \ell(\ell+1)\right] \quad , \quad \ell = 0, L \quad . \tag{8}$$

It can be shown that if one uses the moments defined by Eq. (8) and a Legendre expansion of degree N-1 in conjunction with Gauss quadrature of order N in 1-D slab geometry calculations, the resulting S_N solutions will be equivalent to P_{N-1} solutions (spherical-harmonic solutions of degree N-1) to the Fokker-Planck equation.[1]

Next, we consider the CSD operator. The first step in obtaining coefficients for this operator is to difference this operator using a first-order forward difference. Neglecting the angular discretization and the AD operator in Eq. (1) and assuming a uniform group structure for simplicity, we obtain:

$$\mu\frac{\partial}{\partial z}\psi(E_g) = \frac{\left[S(E_{g-1})\,\psi(E_{g-1}) - S(E_g)\,\psi(E_g)\right]}{\Delta E} \quad , \tag{9}$$

where g is the energy group index, g=1 corresponds to the highest energy group, E_g denotes the midpoint energy for group g, and ΔE denotes the group width. Next we relate the multigroup and discrete fluxes as follows:

$$\psi_g = \psi(E_g)\,\Delta E \quad . \tag{10}$$

Using Eq. (10), we transform Eq. (9) from the differential to the multigroup basis:

$$\mu\frac{\partial}{\partial z}\psi_g = \frac{\left[S_{g-1}\psi_{g-1} - S_g\psi_g\right]}{\Delta E} \quad . \tag{11}$$

Finally, we re-write Eq. (11) in the following way:

$$\mu\frac{\partial}{\partial z}\psi_g + \left(\frac{S_g}{\Delta E}\right)\psi_g = \int_{-1}^{+1}\left(\frac{S_{g-1}}{\Delta E}\right)\delta(\mu_0 - 1)\,\psi_{g-1}(\mu')\,d\mu' \quad . \tag{12}$$

Equation (12) is analogous in form to Eq. (2). Thus, the coefficients for the CSD operator can be obtained by direct comparison of Eqs. (2) and (12). Recalling that the Legendre moments of the delta-function are all unity, we obtain:

$$\sigma_{r,g} = \frac{S_g}{\Delta E} \quad , \tag{13a}$$

$$\begin{aligned}\sigma_{k\to g,\ell} &= \frac{S_{g-1}}{\Delta E} \quad , \quad \ell = 0, L \quad , \quad for\ k = g-1 \quad , \\ &= 0 \quad , \quad otherwise \quad ,\end{aligned} \tag{13b}$$

where $\sigma_{r,g}$ denotes the effective removal cross section for group g. This approximation is completely equivalent to the forward-difference approximation as long as the truncated Legendre expansion for the delta-function is "exact." That is to say that the scattering kernel constructed from the truncated delta-function expansion must act as the identity:

$$\sum_{\ell=0}^{L}(2\ell+1)\,\Phi_{k,\ell}P_\ell(\mu_m) = \psi_{k,g} \quad . \tag{14}$$

It can be shown that if Legendre expansions of degree N-1 are used in conjunction with an N point Gauss quadrature in either 1-D slab or spherical geometries, Eq. (14) will be satisfied.

III. LIMITATIONS OF MULTIGROUP FOKKER-PLANCK REPRESENTATIONS

The derivations of the preceeding section demonstrate the basic approach that is taken to derive multigroup approximations to Fokker-Planck operators. These approaches are useful, but limited. For instance, the CSD operator representation requires that Gauss quadrature be used. Since Gauss quadrature only exists for 1-D slab and spherical geometries, this representation can only be used in these geometries. Although it is not obvious, the AD operator representation cannot be expected to be accurate under all circumstances unless Gauss quadrature is used. Thus, further extensions of this approach clearly require an improved quadrature treatment. We have developed such a treatment and it is called the Galerkin quadrature method.[5,6] We shall not describe this method in detail here. Instead, we simply note that it offers many advantages relative to the standard quadrature method. Most importantly, it can be applied in both one-dimensional and multi-dimensional problems, and all "Galerkin quadratures" give an exact treatment for straight-ahead delta-function scattering when they are used in conjunction with Legendre expansions of appropriate degree. Thus, the Galerkin quadrature method allows us to use our multigroup BFP approach in all geometries. Finally, we note that it can be important to use Galerkin quadrature whenever highly forward-peaked scattering is present in a problem because it has been found that standard quadrature techniques can lead to unstable scattering matrices under such conditions.[6]

We have derived a first-order approximation to the CSD operator, but higher-order approximations can be used. In particular, the second-order diamond-difference scheme can be applied to the CSD operator and represented in multigroup form.[7] When this is done, certain of the effective group-to-group transfer coefficients are negative. These coefficients appear in such a way that they do not interfere with the convergence of the standard source iteration method, but they can cause problems with the negative flux fixup schemes that are implemented in many discrete-ordinates codes. Thus it is best to perform Fokker-Planck calculations with higher-order spatial difference schemes such as the linear-discontinuous scheme employed in the ONETRAN[8] code, that can be used without negative flux fixup. The linear-discontinuous differencing scheme can also be applied to the CSD operator and represented in multigroup form. However, this approximation not only leads to negative coefficients but to upscatter as well.[9] Unfortunately, the infinite-medium spectral radius of the outer iteration operator is unity with this type of upscatter, and the convergence rate in most practical problems is unacceptably slow. A synthetic acceleration scheme has been developed which reduces the spectral radius to 0.1,[9] but this acceleration scheme applies only to the upscatter resulting from the LD-CSD operator. Since it cannot be applied to general types of upscatter, it is not suitable for a general purpose S_n code. Thus, the best approximation to the CSD operator that one can obtain with standard S_n codes is the diamond difference approximation. If one is willing to explicitly include the CSD operator in an S_n code and modify the basic algorithm, the LD CSD operator

can be efficiently solved by treating it like an extra spatial derivative and explicitly sweeping the space-angle-energy mesh.[10]

If the stopping power in Eq. (1) is small and the system is optically thick, the spectral radius of the inner iteration process approaches unity. Thus, acceleration is required under these circumstances. In the limit as the scattering becomes increasingly forward-peaked, standard diffusion-synthetic acceleration becomes ineffective.[11] Improved performance can be obtained by using the P_1 equations as the low-order equations in the synthetic scheme rather than the diffusion equation. This approach represents a straightforward modification of the standard DSA scheme and is referred to as two-moment DSA. This nomenclature arises from the fact that only the zero'th moment of the scattering source is accelerated in standard DSA, but both the zero'th and first moments are accelerated in the two-moment scheme. Like standard one-moment DSA, two-moment DSA becomes ineffective in limit as the scattering becomes increasingly forward-peaked, but two-moment DSA is always significantly more effective than one-moment DSA in the forward-peaked limit.[11] Thus, while two-moment DSA does represent a significant improvement relative to standard DSA, it does not represent a complete solution to the problem of accelerating the S_n equations with highly anisotropic scattering. Testing of the two-moment DSA scheme has shown that negative flux fixup schemes are much more likely to destabilize the DSA algorithm if the scattering is very forward-peaked rather than isotropic.[11] This difficulty can be avoided by using higher-order difference schemes that do not require negative flux fixup. However, DSA with higher-order spatial difference schemes presents a problem in itself because the derivation of the spatially-differenced diffusion equation from the spatially-differenced S_n equations (required to ensure unconditional stability of the DSA method) can be quite difficult even in 1-D slab geometry.[12] To avoid this difficulty, an S_2-synthetic acceleration method for the 1-D S_n equations has been developed.[13,14] The central idea of this method is straightforward. Rather than use the P_1 equations directly as the low-order equations in the synthetic scheme, use a similarity transformation to put the P_1 equations in an S_2 form and difference the resulting S_2 equations the same way that the S_n equations are differenced. Consistency between the spatial differencing of the S_n equations and the low-order equations is thus trivially achieved. Although it is considerably more expensive to directly solve the S_2 equations than the diffusion equation, the 1-D S_2 equations are relatively inexpensive to directly solve. For instance, the diffusion equation derived from the S_n equations with linear-discontinuous spatial differencing gives a three-diagonal matrix equation with one unknown per spatial cell edge, whereas the S_2 equations with linear-discontinuous spatial differencing give a seven-diagonal matrix equation with four unknowns per spatial cell.

The moment representation for the AD operator can yield negative angular flux solutions under certain circumstances. These negative angular fluxes are usually sufficiently small that they do not affect the accuracy of the scalar flux solution. But if accurate angular fluxes in all directions are required, these negative angular fluxes can present a problem. One-dimensional slab and spherical geometry finite-difference schemes for the AD operator have been developed which are exact in the diffusion limit and give unconditionally positive angular flux solutions.[15] However,

finite-difference AD operators cannot be represented with a diagonal matrix in the Legendre basis, thus they cannot be represented in terms of effective cross-section moments. These, then, can only be implemented in S_n codes through modification of the codes. Furthermore, the development of AD differencing schemes for standard multidimensional triangular quadrature sets is not straightforward. Conversely, the moment representation for the AD operator is very versatile in that it can be applied (in conjunction with Galerkin quadrature) in multiple dimensions.

IV. MODIFICATIONS TO ONETRAN

We have implemented the Galerkin quadrature method and the S_2-synthetic acceleration method in the discrete ordinates code, ONETRAN.[8] We stress that although these methods were developed for BFP calculations, they represent general S_n methods that can be applied to standard neutronic and photonic calculations as well. We have also implemented a new angular differencing scheme for the streaming operator in ONETRAN that eliminates the classic "flux-dip" problem.[16] However, this improvement is of much greater significance for neutronics calculations than for charged-particle calculations.

V. COMPUTATIONAL EXAMPLES

In this section we present coupled electron-photon transport calculations performed with the new version of ONETRAN. The multigroup BFP data used in the calculations was generated with the CEPXS code.[17] This code was developed in collaboration with Dr. Leonard J. Lorence, Jr. of Sandia National Laboratories. All calculations presented in this section were performed by Dr. Lorence in support of experimental projects. Thus, realistic rather than ideal calculations are presented.

The first problem considered consists of "fission-spectrum" electrons isotropically-incident from the left upon a 2-cm-thick aluminum slab. The "fission spectrum" is that characteristic of beta particles emitted by fission products and contains electrons with energies from about 8 MeV to 50 keV. The ONETRAN calculation for this problem was carried out with 50 spatial cells, S_8 Gauss quadrature, P_7 cross-section expansions, 50 electron groups linearly spaced from 8 MeV to 10 keV, and 30 similarly spaced photon groups. For comparison, a Monte Carlo calculation was performed with the ITS-TIGER code.[18] A sufficient number of Monte Carlo histories was run to obtain a one-sigma relative deviation of no more than 20 percent in the energy deposited in each spatial cell. The energy deposition profiles calculated with the discrete ordinates and Monte Carlo codes are compared in Fig. 1. The agreement is excellent. However, the ONETRAN calculation required approximately 37 minutes of CPU time on a VAX 11/780 computer whereas the TIGER calculation required approximately 1230 minutes of CPU time on the same computer. Thus, ONETRAN/CEPXS gives the same accuracy as the Monte Carlo code, but is approximately 35 times faster for this problem.

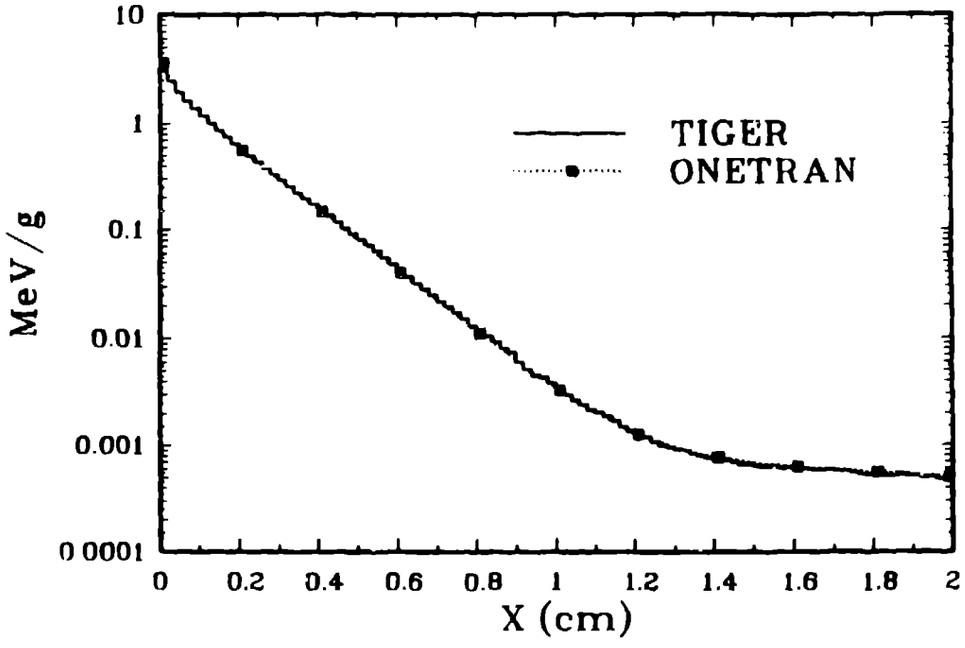

Fig. 1. Energy Deposition Profile for Fission Electrons Isotropically Incident Upon a Slab of Aluminum.

The second problem consists of the same spectrum of electrons isotropically incident from the left upon a 1-D slab model of a shielded integrated circuit chip. This model is referred to as the RADPAK model.[19] The RADPAK geometry is shown in Fig. 2. The energy deposited in the silicon region per electron entering the slab was calculated with both ONETRAN and ITS-TIGER. The ONETRAN calculation gave 5.92×10^{-5} MeV and ITS-TIGER gave $5.7 \pm 0.3 \times 10^{-5}$ MeV. Note that the calculations agree to within the one-sigma deviation quoted for the Monte Carlo calculation. The ONETRAN calculation required approximately 62 minutes of CPU time on a VAX 11/780 computer and the TIGER calculation required approximately 1835 minutes. Thus, ONETRAN/CEPXS gives the same accuracy as TIGER for this problem, but is about 30 times faster.

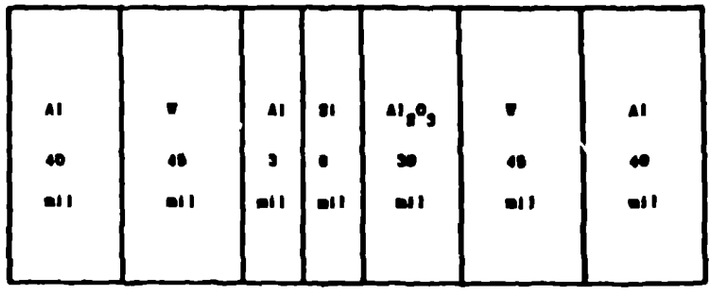

Fig. 2. RADPAK 1-D Geometry.

The third problem is identical the the second except that we performed an adjoint calculation with ONETRAN to calculate the energy deposition in the silicon as a function of energy for both electrons and photons isotropically incident from the left. The group-dependent response values are plotted in Fig. 3. Each histogram corresponds to a group. Let R_g^e and R_k^p denote the electron and photon responses associated with electron group g and photon group k, respectively. The energy deposited in the silicon per electron in group g entering the slab is given by $4R_g^e$. Similarly, the energy deposited in the silicon per photon in group k entering the slab is given by $4R_k^p$. Thus, the response curves obtained with a single ONETRAN adjoint calculation allow one to obtain the energy deposited in the silicon for an arbitrary electron or photon source spectrum. This adjoint calculation required about 90 minutes of CPU on a VAX 11/780 computer. Standard coupled electron-photon Monte Carlo codes such as ITS-TIGER do not offer an adjoint capability.

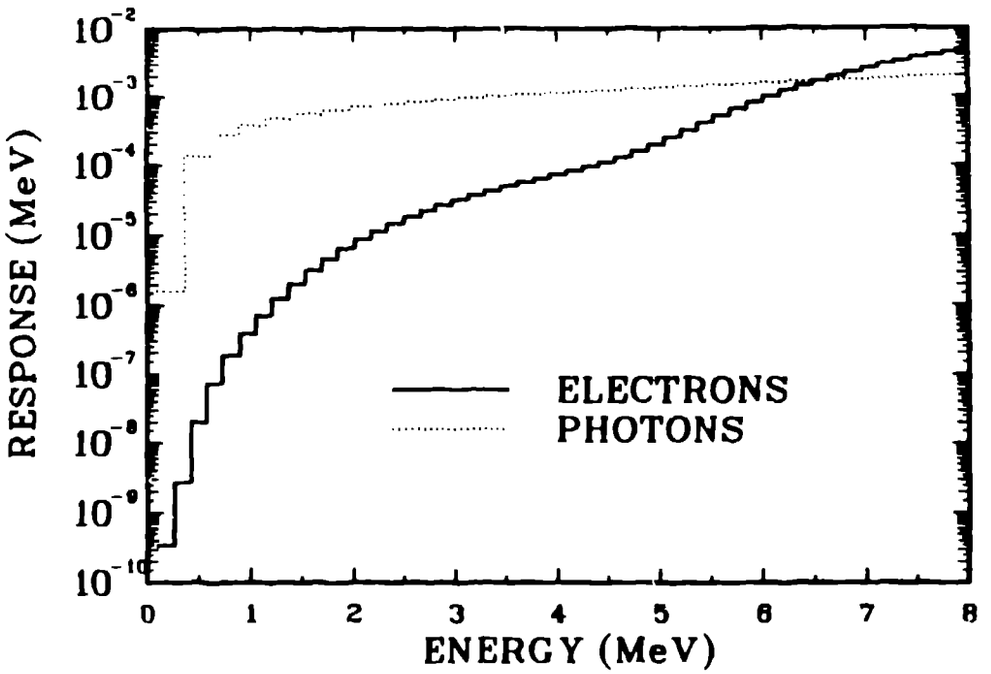

Fig. 3. Adjoint Solutions for Electrons and Photons Isotropically Incident Upon the RADPAK Configuration from the Left. The dose to the silicon chip in the RADPAK configuration can be calculated for any source spectrum of electrons and/or photons with these curves.

The fourth problem consists of a plane wave of 100-keV photons incident from the left upon a slab of graphite. We have calculated the photoemission efficiency (electrons emitted per photon entering the slab) at the right face of the slab with both ONETRAN and ITS-TIGER as a function of slab thickness. The efficiencies are plotted in Fig. 4. The agreement between the calculations is excellent. The CPU times required by each code as a function of slab thickness are plotted in Fig. 5. The calculations were performed on a CRAY XMP. Note that the ONETRAN CPU

times are constant at about 60 seconds whereas the ITS-TIGER CPU times steadily increase from about 100 seconds to about 10000 seconds. Thus, ONETRAN gives the same accuracy as ITS-TIGER but is over 100 times faster. A constant CPU time was achieved with ONETRAN by using the same total number of spatial cells in each calculation and varying the spacing such that the right edge of the slab was always well resolved. The ITS-TIGER calculations were carried out with a special version of TIGER called IFS-TIGER, which was developed specifically for this type of problem.

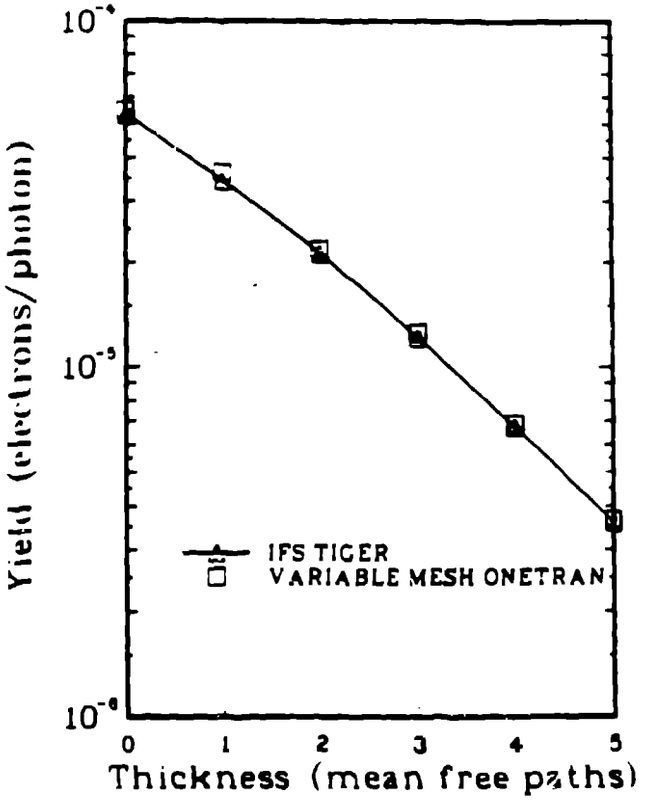

Fig. 4. Transmitted Electron Photoemission Yield as a Function of Slab Thickness for 100 keV Electrons Normally Incident Upon a Slab of Graphite. The slab thickness is given in photon mean-free-paths.

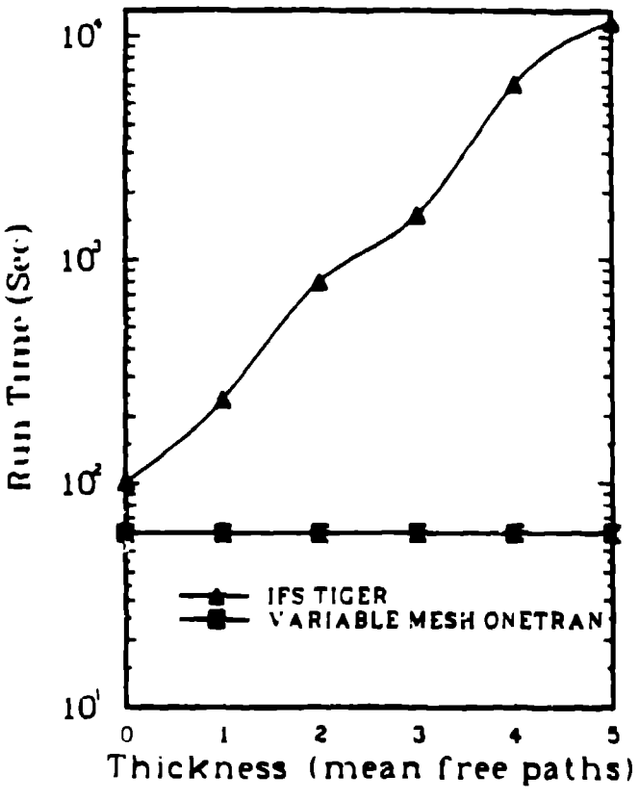

Fig. 5. CPU Times for Monte Carlo and S_n Methods for Photoemission Calculations as a Function of Graphite Slab Thickness.

The fifth problem consists of a plane-wave of Co-60 gamma-rays incident upon a two-layer slab of lithium-fluoride and lead. We have calculated the energy deposition profile for this problem using both ONETRAN and ITS-TIGER. The corresponding curves are plotted in Fig. 6. The agreement between the calculations is quite good. The ONETRAN calculation required about 2 minutes of CPU time on a CRAY-XMP and ITS-TIGER required about 20 minutes of CPU time. This calculation was performed with a version of ITS-TIGER that was modified specifically for this problem to achieve the highest efficiency possible. The charge deposition was also calculated for this problem with ONETRAN and ITS-TIGER. However, we were unable to obtain reasonable statistical accuracy with ITS-TIGER after an hour of CPU time on a CRAY-XMP. All charge depositions values were estimated to have one-sigma relative deviations of over 100 percent. It was estimated that at least 10 hours of CPU time would be required to obtain reasonable statistical accuracy. Thus, even though the Monte Carlo method is reasonably efficient for calculating the energy depostion in this problem, it is prohibitively expensive for calculating charge deposition. Conversely, ONETRAN provides both the energy and charge depostion profiles with equal efficiency. Considering the results which

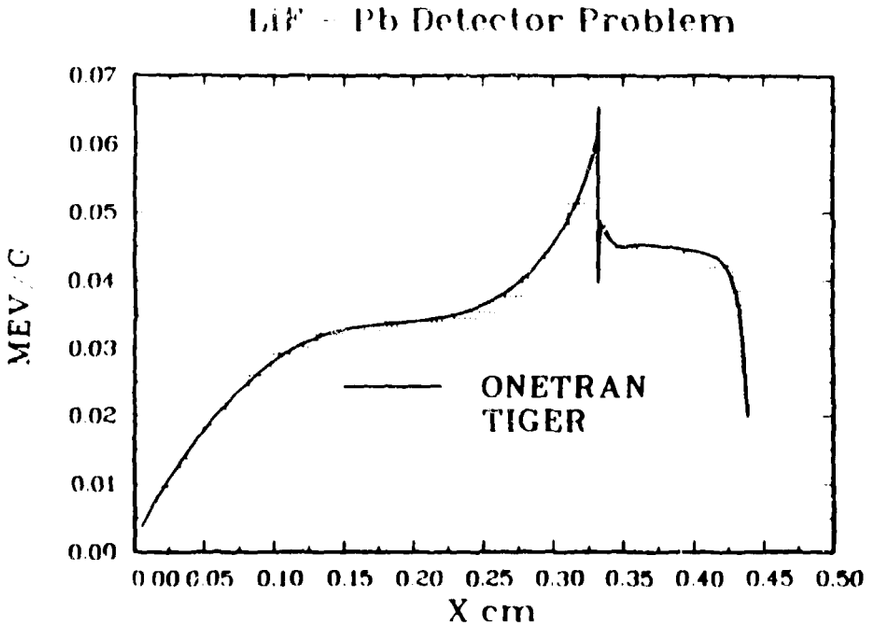

Fig. 6. Dose Profile for Co-60 Gamma Rays Normally Incident from the Left Upon a Sandwich of LiF and Pb. The left and right portions of the slab are LiF and Pb, respectively.

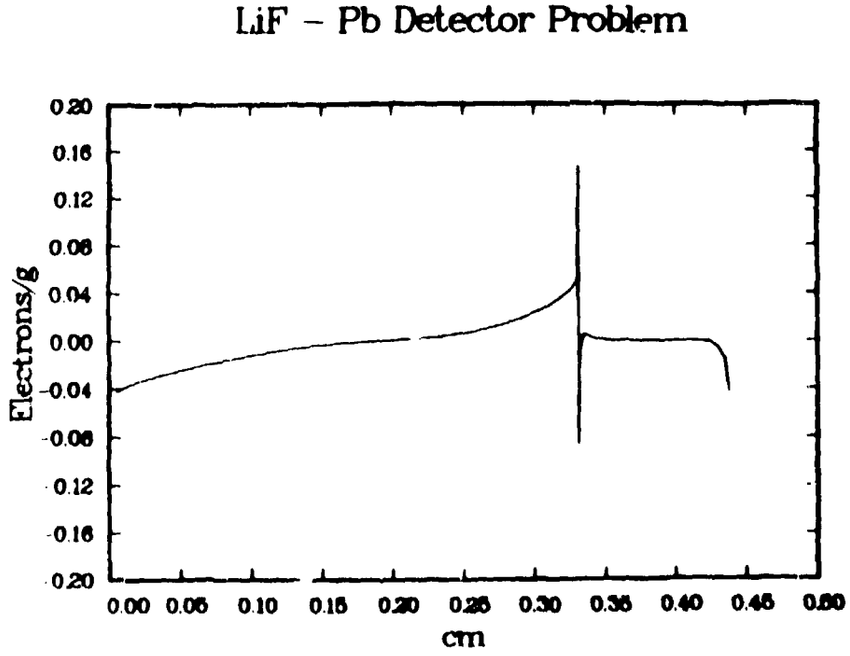

Fig. 7. Charge Profile for Co 60 Gamma Rays Normally Incident from the Left Upon a Sandwich of LiF and Pb. The left and right portions of the slab are LiF and Pb, respectively.

we have obtained, it seems quite fair to expect that ONETRAN would run on the order of 1000 times faster than ITS-TIGER on this charge deposition calculation, however, we cannot confirm this because of the expense of performing the Monte Carlo calculations. The charge deposition profile calculated with ONETRAN is plotted in Fig. 7. Note the rapid variation of the solution in the boundary layers near the material interface and the outer faces. A very non-uniform spatial mesh was used to resolve this behavior.

VI. CONCLUSIONS

Our results clearly demonstrate that coupled electron-photon BFP calculations can be efficiently and accurately performed with standard discrete-ordinates codes designed only to solve the Boltzmann equation. For a large class of realistic problems, the discrete-ordinates method is very much more efficient than the Monte Carlo method. In the near future, we hope to apply our BFP method to other types of transport calculations. In particular, we intend to compare the discrete ordinates method with standard Monte Carlo methods for ion transport problems of interest to materials scientists.

The accuracy of the approximations for Fokker-Planck operators that can be used with standard discrete ordinates codes is limited by the restriction that these approximations be representable in multigroup-Legendre form. These approximations appear to be adequate for a wide range of coupled electron-photon transport problems, but greater accuracy is desirable for other types of calculations. This can only be achieved by explicitly writing discrete ordinates codes to solve the Boltzmann-Fokker-Planck equation rather than just the Boltzmann equation. We believe that the results that we have obtained for coupled electron-photon BFP calculations justifies the development of such codes. In the near future, we hope to develop such a code for 1-D slab geometry calculations and use it to test the accuracy of our BFP methods for ion transport calculations of interest to the materials science community.

REFERENCES

1. J. E. Morel, *Nucl. Sci. Eng.*, 79, 340 (1981).

2. K. Przybylski and J. Ligou, *Nucl. Sci. Eng.*, 81, 92 (1982).

3. M. Caro and J. Ligou, *Nucl. Sci. Eng.*, 83, 242 (1983).

4. E. E. Lewis and W. F. Miller, Jr., *Computational Methods of Neutron Transport*, John Wiley and Sons, Inc., New York (1984).

5. J. E. Morel, *Trans. Am. Nucl. Soc.*, 39, 459 (1981).

6. J. E. Morel, "A Hybrid Collocation-Galerkin-S_n Method for Solving the Boltzmann Transport Equation," submitted to *Nuclear Science and Engineering.*

7. J. E. Morel, *Nucl. Sci. Eng.*, 91, 324 (1985).

8. T. R. Hill, "ONETRAN: A Discrete Finite Element Code for the Solution of the One-Dimensional Multigroup Transport Equation," LA-5990-MS, Los Alamos National Laboratory (1975).

9. Maximo S. Lazo and J. E. Morel, *Nucl. Sci. Eng.*, 92, 98 (1986).

10. J. J. Honrubia and J. M. Aragones, *Nucl. Sci. Eng.*, 93, 386 (1986).

11. J. E. Morel, *Nucl. Sci. Eng.*, 82, 34 (1982).

12. Edward W. Larsen, *Nucl. Sci. Eng.*, 82, 47 (1982).

13. L. J. Lorence, Jr., E. W. Larsen, and J. E. Morel, *Trans. Am. Nuc. Soc.*, 52 417 (1986).

14. L. J. Lorence, Jr., E. W. Larsen, and J. E. Morel, "An S_2 Synthetic Acceleration Scheme for the One-Dimensional S_n Equations," to be submitted to *Nuclear Science and Engineering.*

15. J. E. Morel, *Nucl. Sci. Eng.*, 89, 131 (1985).

16. J. E. Morel and G. R. Montry, *Transport Theory and Statistical Physics*, 13, 615 (1984).

17. L. J. Lorence, Jr., and J. E. Morel, "CEPXS: A Coupled Electron-Photon BFP Multigroup-Legendre Cross-Section Generation Code," to be published as a Sandia National Laboratories report.

18. J. A. Halbleib and T. A. Mehlhorn, "ITS: The Integrated TIGER Series of Coupled Electron/Photon Monte Carlo Transport Codes," SAND84 0573, Sandia National Laboratories (1984).

19. M. Merker, P. Schmid, J. Spratt, and D. Strobel, "RAD-PAK Radiation Shielding for IC's at the Package Level," AFWL-TR-83-117, Air Force Weapons Laboratory (1984).